Journal of
NANOSTRUCTURES
JNS
NANOSTRUCTURES
JNS.kashanu.ac.ir

Electrosynthesis of Polyaniline-TiO_2 Nanocomposite Films on Aluminum Alloy 3004 Surface and its Corrosion Protection Performance

M. Shabani-Nooshabadi*, S. M. Ghoreishi, Y. Jafari

Department of Analytical Chemistry, Faculty of Chemistry, University of Kashan, Kashan, I.R. Iran.

Article history:
Received 2/4/2013
Accepted 28/5/2013
Published online 1/6/2013

Keywords:
Polyaniline
TiO_2
Nanocomposite
Aluminum alloy 3004
Corrosion

**Corresponding author:*
E-mail address:
m.shabani@kashanu.ac.ir
Phone: 98 3612395

Abstract

The direct synthesis of polyaniline-TiO_2 nanocomposite coatings on aluminum alloy 3004 (AA3004) surface has been investigated by using the galvanostatic method. The synthesized coatings were characterized by FT-IR, SEM-EDX, SEM and AFM. Optical absorption spectroscopy reveals the formation of the emeraldine oxidation state form of polyaniline-TiO_2 nanocomposite. The corrosion performances of polyaniline-TiO_2 nanocomposite coatings were investigated in 3.5% NaCl solution by Tafel polarization and Electrochemical Impedance Spectroscopy (EIS) methods. The corrosion rate of polyaniline-TiO_2 nanocomposite coating on AA3004 was found ~260 times lower than bare AA3004 and corrosion potentials of these coatings have shifted to more positive potentials (105 mV). The results of this study clearly ascertain that the polyaniline-TiO_2 nanocomposite coating has outstanding potential to protect the AA3004 against corrosion in a chloride environment.

1. Introduction

Aluminum alloys have applications in aerospace, transportation and beverage industries because of their lightweight and high strength properties [1]. Aluminum, a very reactive metal, forms a thin solid protecting film of oxide which prevents the further corrosion of the material. However, in contact with solutions containing complex agents (i.e. halides), aluminum undergoes localized corrosion various attempts have been made to study the influence of different ions on the electrochemical behavior and pitting corrosion of Al and its alloys [2, 3].

Protecting aluminum by covering its surface with an organic coating is a good way for taking

advantages of the mechanical property of the metal while protecting it from corrosion. Adhesion of these organic coatings on aluminum is very poor and needs some pretreatment like chromating. Due to the carcinogenic nature of chromate conversion coatings, there is a high demand for an environmentally friendly surface treatment [4-9].

During the last two decades, attention has been focused on conducting polymers, particularly aromatic polymers such as polyaniline and its derivatives and polypyrrole [10- 16]. Due to these interesting physical properties, conducting polymers exhibit a broad spectrum of potential industrial applications in various fields, such as electronic and electro chromic equipment, photochemical cells, rechargeable batteries, separation membranes, sensors and anticorrosive coatings [17- 19].

Among the family of conducting polymers, polyaniline and its derivatives have received most attention due to their environmental and chemical stability and their ability to switch reversible from insulating state to conducting state [20]. However, the in ability of polyaniline to dissolve in common organic solvents has restricted its use in certain fields. The addition of a functional group as a substituent to the polyaniline backbone results in a material, which is more soluble and easily process able. It also possesses the appealing characteristics of polyaniline. While the incorporation of a substituent will increase its solubility and enhance the stability of the polymer product, the electrical conductivity is decreased, due to the increase in electronic localization or reduction in π-conjugation. Despite this, much work remains to be done to understand the properties of these substituted polyaniline so as to apply them technologically [21- 26].

On the mechanism of corrosion protection by polyaniline, it has been well established that polyaniline has both barrier and electrochemical protection effects. The electrochemical protection is caused by increasing of the corrosion potential and forming of a protective passive layer on metal surface due to redox catalytic properties [27]. However, to enhance the efficiency of corrosion protection by the polyaniline coating, the adhesion, mechanical properties and barrier effect of the polyaniline coating must be improved. Several strategies have been used to increase the effectiveness of polyaniline as an anticorrosive coating on metals [28].

The incorporation of inorganic fillers into conducting polymer matrices by electrochemical polymerisation processes has also been studied [29]. Zhu and Iroh [30] electrosynthesised polyaniline in the presence of TiO_2, ZrO_2 and SiO_2 nanoparticles on aluminum alloy 2024. The potentiodynamic polarization behavior suggested a beneficial effect of the fillers on the corrosion resistance provided by polyaniline coatings, although no mechanistic inthe formation was provided. Lenz et al [31], electrosynthesised polypyrrole on mild steel in the presence of TiO_2 particles. The polypyrrole-TiO_2 nanocomposite films showed improved performance compared with the polypyrrole films that was attributed to the reduced porosity of the polymer through filling by TiO_2 particles. The main objective of the present study is to electropolymerize polyaniline-TiO_2 nanocomposite on AA3004 electrode from aqueous oxalic acid solution via the galvanostatic method by optimizing the

electrodeposition conditions for direct electrochemical synthesis. According used the method for the synthesis of polymers it can be said, that the work is new [32-35].

The aqueous electrochemical process is an environmentally friendly and efficient technique used to process conducting polymer coatings. It is widely preferred because of its simplicity and it can be used as a one-step method to form coating on metal substrates. It allows efficient control of the chemical and physical properties of the coatings, and it can also be easily adapted to large-scale production [36].

In this work, we have electrochemical synthesized strongly adherent polyaniline-TiO_2 nanocomposite coatings on aluminum alloy 3004 by using the direct electrochemical galvanostatic method. The corrosion resistant properties of polyaniline-TiO_2 nanocomposite coated samples were evaluated by polarization and EIS techniques in 3.5% NaCl. We also present the characterization of the coatings by Fourier transform infrared spectroscopy (FTIR), Energy dispersive X- ray (EDX) patterns, scanning electron microscopy (SEM) and Atomic force microscopes (AFM).

2. Experimental procedure

2.1. Apparatus and materials

Aluminum alloy 3004, of nominal composition given in Table 1, was used as the substrate. The metal sheet was cut into rectangular samples of 1cm^2 area and 0.6 mm thickness soldered with Al-wire for an electrical connection and mounted onto the epoxy resin to offer only one active flat surface exposed to the corrosive environment. Navard Aluminum Manufacturing Group (Iran) supplied the AA3004 sheet. P-25 TiO_2 nanoparticles purchased from Degussa AG (Germany) that size range of the TiO_2 nanoparticles was 25-75 nm, other chemicals were purchased from Merck.

Table. 1. Nominal chemical composition of the aluminum alloy 3004.

Elemen	Si	Fe	Cu	Mn	Mg	Zn	Al
Wt%	0.30	0.70	0.25	1.5	0.8	0.25	96.20

Aniline was freshly distilled and stored in the dark. All solutions were prepared with doubly distilled water. For each run, a freshly prepared solution and a cleaned set of electrodes were used and all experiments were carried out at room temperature. Electrochemical experiments and corrosion tests were carried out using an AUTOLAB PGSTAT 30 potentiostat/galvanostat (Eco Chemie, Utrecht, Netherlands) connected to a Pentium IV personal computer through an USB electrochemical interface. Pre-treated AA3004 was used as working electrode in the conventional three- electrode cell. For characterization of electropolymerized layers the FT-IR spectra polyaniline-TiO_2 nanocomposite over AA3004 was obtained and compared to polyaniline and TiO_2 nanoparticles using a Shimadzu Varian 4300 spectrophotometer in KBr pellets.

The morphology of the electropolymerized polyanilin-TiO_2 nanocomposite coatings onAA3004 was analyzed using a SERON model AIS-2100 scanning electron microscope (SEM) instrument operating at 10 kV equipped with an energy dispersive X-ray (EDX) spectroscopy. The samples were mounted on a double-sided adhesive carbon disc and sputter

coated with a thin layer of gold to prevent sample charging problems.

2.2. Pretreatment of AA3004

Before each experiment, the working electrode was abraded with a sequence of emery papers of different grades (320, 400, 800, 1000, 1200, 2000 and 2200) and substrates were degreased with acetone and then dipped in 5%NaOH solution for 120 s to activate the surface. After this stage, the samples were cleaned with detergent powder to remove the black colored smudge formed over the surface and were washed thoroughly with running water and dipped in a concentrated HNO_3 solution for 30 s. The samples were then washed with distilled water and used for electropolymerization.

2.3. Electropolymerization of polyaniline-TiO_2 coatings on AA3004

As a typical procedure for the preparation of polyaniline-TiO_2 nanocomposite coatings with 1 wt% of TiO_2 nanoparticles, a mixture of 0.5 M of oxalic acid and 0.1 M of aniline monomer, with 1 wt% of dispersed TiO_2 nanoparticles prepared. Subsequently, the obtained solution was ultrasonic for 15 min in order to increase its uniformity.

Electropolymerization was carried out by galvanostatic method from 15 mL of the prepared solution. Electropolymerization of polyaniline-TiO_2 over AA3004 surface was also carried out by keeping a fixed current for certain duration of time. In this regard, three current densities 5, 10 and 15 $mAcm^{-2}$ were attempted and the corresponding potential transients were recorded for a period of 1800 s. Pre-treated AA3004 was used as the working electrode in the conventional three electrode assembly, having a graphite rod as the counter electrode and a saturated calomel electrode (SCE) as the reference electrode.

2.4. Corrosion tests

The AA3004 samples with electropolymerized polyaniline-TiO_2 nanocomposite coatings were evaluated for their corrosion resistance properties in 3.5% NaCl by Tafel polarization and electrochemical impedance spectroscopy. The polyaniline-TiO_2 nanocomposite coated AA3004 was used as the working electrode in the conventional three-electrode assembly, having a platinum sheet as the counter electrode and a saturated calomel electrode (SCE) as the reference electrode. The working electrode was first immersed in the test solution for 1 h to establish a steady state open circuit potential (OCP).

In the case of Tafel polarization, the potential was scanned at ±200mV vs. SCE versus OCP with a scan rate the 0.1 mVs^{-1}. The corrosion potential (E_{corr}) and the corrosion current (I_{corr}) were obtained from the Tafel plots and using the general purpose electrochemical software (GPES). In the case of electrochemical impedance spectroscopy of 10 mV amplitude and various frequencies from 100 kHz to 0.01 Hz at open circuit potentials were impressed to the coated AA3004 in the electrode surface 1 cm^2. A Pentium IV-powered computer and frequency response analysis (FRA) software were applied for analyzing impedance data.

3. Results and discussion

3.1. Electrosynthesis of polyaniline-TiO_2 nanocomposite

The E-t transient curve was obtained during the the formation of polyaniline-TiO_2 nanocomposite coatings on AA3004 for three different applied current densities 5, 10 and 15 mA cm^{-2} deposition time of 1800 s that is shown in Fig. 1. As seen in Fig. 1, the polymerization potential values were about 16 V versus SCE for all applied current densities, but induction time before the passive layer was built up decreased with increasing applied current densities.

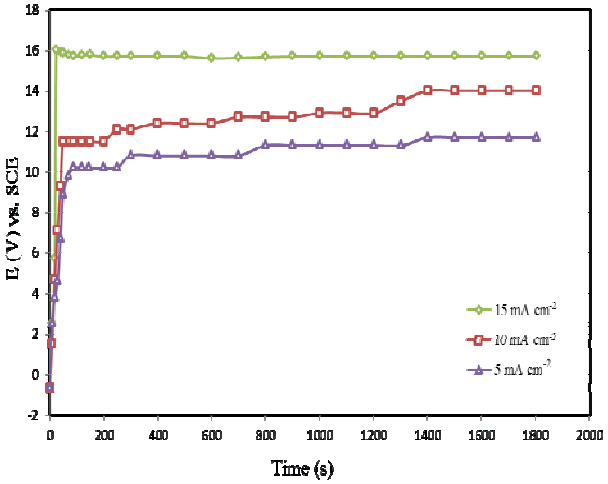

Fig. 1. E-t curves under galvanostatic polymerization conditions in 0.5 M oxalic acid solution containing 0.1 M aniline and 1 wt% dispersed TiO_2 nanoparticles for AA3004 electrode at various current densities.

The coatings of homogeneous appearance were obtained at various applied current densities. The time to reach the maximum value is different for the applied current densities that it is nominated as induction time and is shown in Fig. 2. At higher applied current densities, the induction times were shorter. Thus, when the applied current density is higher, the substrate can be covered by the passive layer in a shorter time [37].

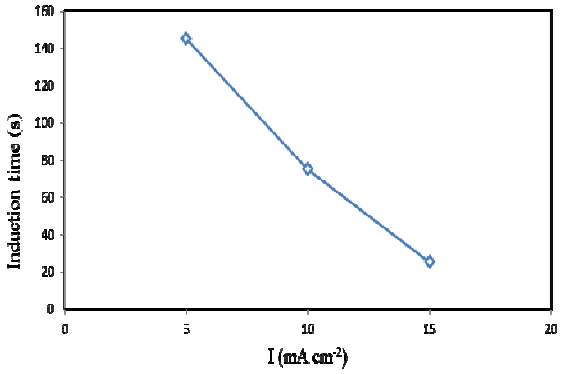

Fig 2. Induction times for applied current densities.

The galvanostatic procedure gave rise to the deposition of green coatings, characteristic of polyaniline in the emeraldine oxidation state (the mechanism is in Fig. 3 [35]), after the coating polyaniline-TiO_2 nanocomposite the formation on the AA3004, the surface was washed with water and ethanol, the coatings weren't separated from the electrode surface and the adhesive remained on the AA3004 surface.

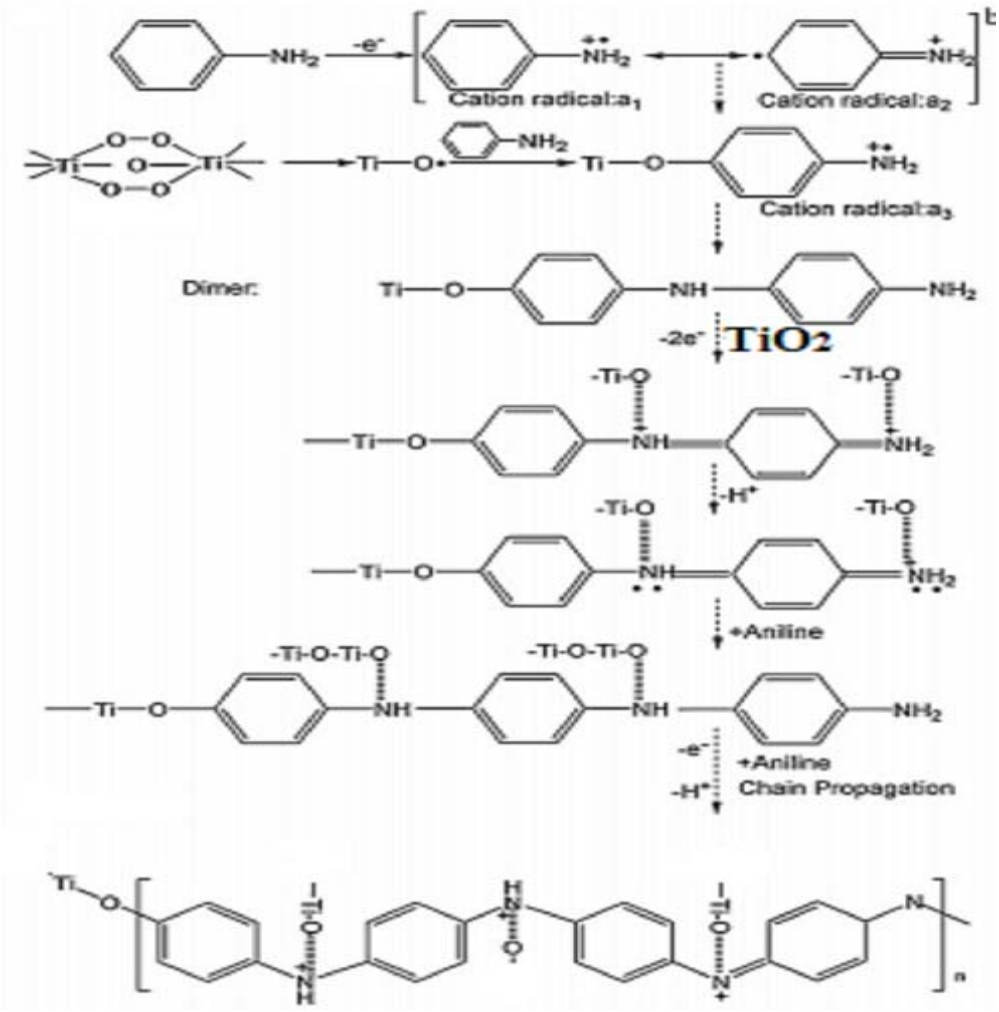

Fig. 3. Electropolymerization mechanism of polyaniline-TiO_2 nanocomposite on AA3004.

3.2. Spectroscopic characterization

The typical FT-IR absorption spectra for TiO_2, pure polyaniline and polyaniline-TiO_2 nanocomposite containing 1 wt% TiO_2 nanoparticles are shown in Fig. 4. The characteristic for pure polyaniline peaks were observed at 3430, 2926, 1490, 1140 and 800 cm^{-1}, in agreement with the literature reported [1].

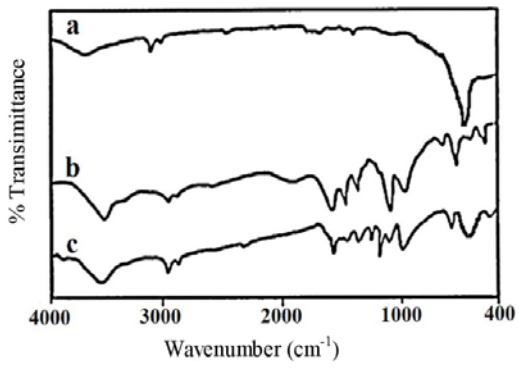

Fig 4. FT-IR spectra (a) TiO_2 nanoparticles, (b) pure polyaniline and (c) the polyaniline-TiO_2 nanocomposite.

In the spectrum of the polyaniline-TiO_2 nanocomposite, characteristic absorbance bands of pure polyaniline and TiO_2 nanoparticles occurred at the following locations: the peak at 3430 cm^{-1} is due to the N- H stretching vibration of secondary amine, the aromatic C-H stretching vibration at about 2926 cm^{-1}, C-N stretching vibration at 1305 cm^{-1} and the in-plane C-H bending at about 1140 cm^{-1} reveal the characteristic bands of pure polyaniline. The peak at about 800 cm^{-1} is characteristic of the para-di substituted aromatic rings that indicate polymer the formation. The bands at approximately 1490 and 1570 cm^{-1} are due to the benzeneoid and quinoid ring units. It was found that the polyaniline film formed by galvanostatic conditions contained both benzenoid and quinoid moieties. The peaks corresponding to stretching vibrations of O-H and bending vibrations of adsorbed water molecules around 3350-3450 cm^{-1} and the broad intense band below 1200 cm^{-1} is due to Ti-O-Ti vibration [28, 38, 39], all of which confirm the presence of TiO_2 nanoparticles in the polyaniline-TiO_2 nanocomposite. Therefore, the FT-IR technique confirms the incorporation of TiO_2 nanparticles in polyaniline matrix that was formed using electropolymerization method for nanocomposite preparation.

3.3. Scanning electron microscopy (SEM) and EDX analysis

Fig. 5 shows SEM micrographs of the polyaniline-TiO_2 nanocomposite samples at current densities 15 mA cm^{-2}. Images show that nanoparticles are uniform, global and slightly agglomerated. Further observation indicates that the morphology of samples is very dense and uniform and may be beneficial to enhancing the corrosion protection due.

The EDX data of polyaniline-TiO_2 nanocomposite containing 1wt% TiO_2 sample is shown in Fig 6. Nano-TiO_2 shows a peak around 2.2-2.5KeV and another intense peak appear at 4.3 and 4.5KeV.Aluminum exist in the surface shows a peak toward 1.5KeV [40], these results confirm that Ti and O exist in the nanocomposite structure on aluminum alloy surface.

3.4. AFM characterization

AFM is a powerful technique to investigative the surface morphology at nano to micro scale and has become a new choice to study the influence of coatings on the generation and the progress of the corrosion at the metal/solution interface.

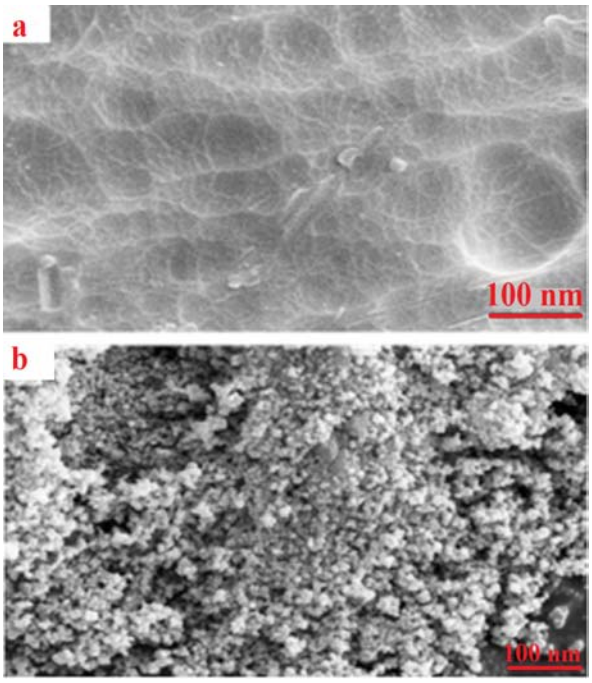

Fig 5. SEM images of the (a) abraded AA3004 and (b) electrosynthesized polyaniline-TiO_2 nanocomposite coated AA3004 for 15 $mAcm^{-2}$.

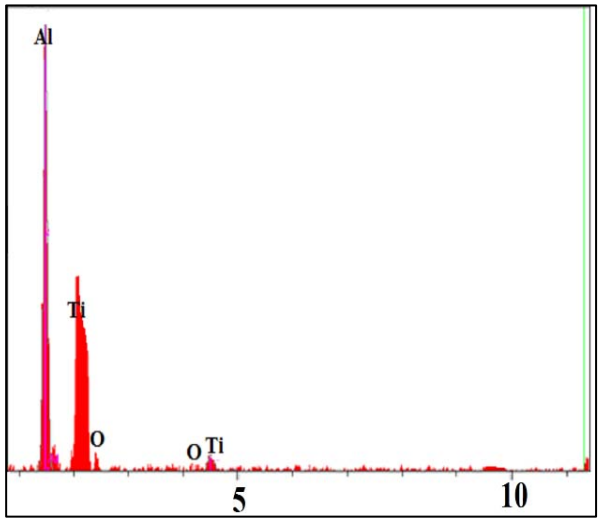

Fig 6. EDX pattern of the electrosynthesized polyaniline-TiO_2 nanocomposite coated AA3004 for 15 $mAcm^{-2}$.

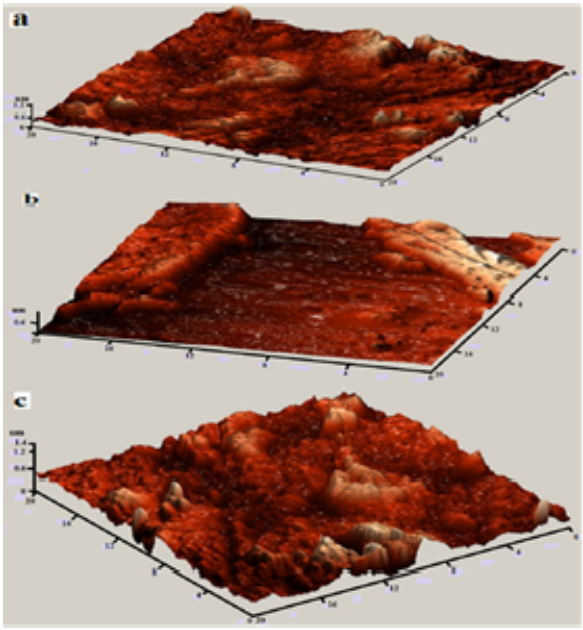

Fig 7. Atomic force micrographs of abraded AA3004 (image a) pre-treated AA3004 after corrosion (image b) and polyaniline-TiO_2 nanocomposite coatings grown by an applied current density of 15 $mAcm^{-2}$ after corrosion (image c).

Fig. 7 shows the typical AFM images of abraded Al (image a), pre-treated Al after corrosion (image b), polyaniline-TiO_2 nanocomposite coatings grown by an applied current density of 15 $mA.cm^{-2}$ after corrosion (image c). A comparison of image c shows that the polyaniline-TiO_2 nanocomposite coating protects the Al, which does not change dramatically.

3.5. Corrosion protection evaluation of the coatings

The corrosion protection performance of polyaniline-TiO_2 nanocomposite coatings synthesized under galvanostatic conditions were examined in an aqueous 3.5 wt% NaCl solution using potentiodynamic polarization and EIS studies.

3.5.1. Tafel polarization measurements

The typical potentiodynamic polarization curve for uncoated AA3004, polyaniline-TiO_2 nanocomposite- coated AA3004 in an aqueous 3.5% NaCl, are shown in Fig. 8. As shown in the curves, the corrosion potential for polyniline-TiO_2 nanocomposite- coated AA3004 has shifted to more positive potentials, about 105 mV vs. SCE higher than the uncoated AA3004 (anodic protection). The electrochemical protection is caused by the increase of the corrosion potential and the formation of a protective passive layer on AA3004 surface due to redox catalytic properties.

The corrosion current density (I_{corr}), corrosion potential (E_{corr}), polarization resistance (R_p), corrosion rate (C_R) and protection efficiency (PE) were determined by extrapolation of the linear portions of the anodic and cathodic Tafel curves from Fig. 8 are presented in Table 2.

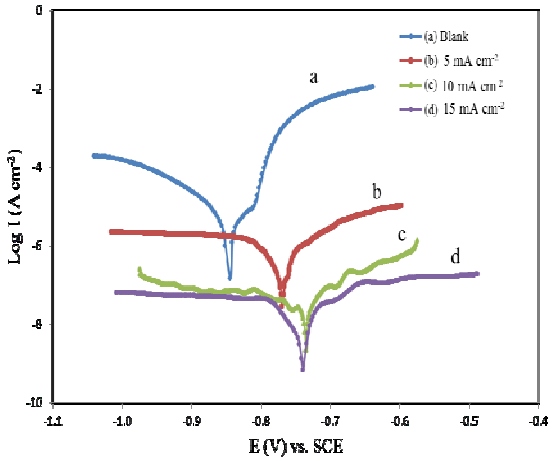

Fig 8. Polarization behavior of electropolymerzied polyaniline-TiO_2 nanocomposite- coated on AA3004 at various current densities ($mAcm^{-2}$) in 3.5% NaCl.

From the measured corrosion current density values, the protection efficiency was obtained from the following equation [41, 42]: $PE = [(I_{corr} - I_{corr(c)}) / I_{corr}]\times 100$ (1). That I_{corr} and $I_{corr(c)}$ are the corrosion current density values in the absence and presence of the coating, respectively.

As it can be seen in Table 2, when the applied current density increases, the protection efficiency (PE) increases, too. But corrosion current densities decrease from 5.2 μA cm^{-2} for uncoated AA3004 to 0.09 μA cm^{-2} for polyaniline-TiO_2 nanocomposite-coated AA3004 under optimal condition. From Table 2 it can be also found that the corrosion rate of Al is significantly reduced as a result of the reduction in I_{corr}. The corrosion rate of the polyaniline-TiO_2 nanocomposite- coated AA3004 is found to be 3.2×10^{-4} mm $year^{-1}$, which is ~ 260 times lower than that observed for bare AA3004.The polarization resistance (R_p) is an important parameter, that ability of coating in prevention of electron exchange in a corrosive environment.

It can be seen that the corrosion current of polyaniline-TiO_2 nanocomposite-coated samples was lower than for polyaniline- montmorrilonite nanocomposite and pure polyaniline-coated samples with comparison of our previous work [28, 43].

Therefore, it was found that the incorporation of TiO_2 nanoparticles in the polyaniline matrix promotes the anticorrosive efficiency of the polyaniline-TiO_2 nanocomposite coating on Al samples. However enhanced corrosion protection by the polyaniline-TiO_2 nanocomposite over the protection by pure polyaniline might result from the nano layers of TiO_2 dispersed in the polyaniline matrix as at filler, that increase of the diffusion path way of corrosive agents such as oxygen gas, hydrogen and chloride ions [44].

The coating porosity is an important parameter, which strongly governs the anticorrosive behavior of the coatings. In this work, the porosity of polyaniline-TiO_2 nanocomposite coatings on AA3004 substrates was determined from potentiodynamic polarization measurements. The porosity of the polyaniline-TiO_2 coating was calculated using the following equation [45]: $P = (R_{puc}/ R_{pc}) \times 10^{-(|\Delta E|/ b_a)}$ (2). Where P is the total porosity, R_{puc} and R_{pc} are the polarization resistance of the uncoated and coated AA3004, respectively. ΔE is the difference between the corrosion potentials and b_a is the anodic Tafel slope for the uncoated AA3004 substrate.

As a result, there is a decrease in the accessibility of the aggressive species to the AA3004 surface and therefore a decrease occurs in the corrosion rate and corrosion current values. Table 2 also shows that with increasing

of applied current density, corrosion protection efficiency will increase.

Table 2. Electrochemical parameters of electropolymerized polyaniline-TiO_2 nanocomposite on AA3004 in aqueous 3.5% NaCl solution under the galvanostatic conditions at different current densities.

Sample	I_{corr} (μAcm^{-2})	E_{corr} (V vs.SCE)	R_p (Ωcm^2)	C_R ($mmyear^{-1}$)	PE%	Porosity%*
Bare*	5.20	-0.842	3.8×10^{2}	8.3×10^{-2}	-	-
5 $mAcm^{-2}$	0.51	-0.764	8.7×10^{3}	2.8×10^{-3}	90.1	0.200
10 $mAcm^{-2}$	0.21	-0.734	3.1×10^{4}	8.7×10^{-4}	95.5	0.020
15 $mAcm^{-2}$	0.09	-0.737	8.3×10^{4}	3.2×10^{-4}	98.2	0.008

(b_a: 0.06 V dec^{-1})*

Table 3. Impedance parameter values of the electrosynthesized polyaniline-TiO_2 nanocomposite extracted from the fit to the equivalent circuit for the impedance spectra recorded in aqueous 3.5% NaCl solution.

Sample	R_s ($\Omega.cm^2$)	C_c ($F.cm^{-2}$)	R_{por} ($\Omega.cm^2$)	R_{ct} ($k\Omega.cm^2$)	C_{dl} ($F.cm^{-2}$)	d* (μm)	PE%
Bare	2.2	4.1×10^{-5}	5.5	3.3	1.3×10^{-5}	-	-
5 $mAcm^{-2}$	14.0	3.1×10^{-6}	73.0	19.7	1.2×10^{-6}	0.16	83.2
10$mAcm^{-2}$	15.1	2.5×10^{-7}	94.0	38.1	2.8×10^{-7}	2.08	91.3
15 $mAcm^{-2}$	17.3	8.2×10^{-8}	102.0	51.2	8.3×10^{-8}	6.36	93.5

* ($\square_0$= 8.85×10^{-12} $F.cm^{-1}$, $\square$ = 5.9, A = 1 cm^2)

3.5.2. Electrochemical impedance measurements (EIS)

In this study, electrochemical impedance spectroscopy was also used to evaluate the corrosion activity variation for AA3004 coated with the polyaniline-TiO_2 nanocomposite. The impedance spectra of the polyaniline-TiO_2 nanocomposite coated AA3004 electrodes at the applied currents density had a similar shape.

The Nyquist impedance plots of uncoated AA3004 and polyaniline-TiO_2 nanocomposite coated AA3004 recorded in an aqueous 3.5% NaCl solution are shown in Fig. 9. These impedance plots were modeled by the equivalent circuit depicted in Fig. 10. The equivalent circuit consists of the electrolyte resistance (R_s), pore resistance (R_{por}), coating capacitance (C_c), charge transfer resistance (R_{ct}) and double layer capacitance (C_{dl}). The R_{ct} is the charge transfer resistance of the area at the metal/coating interface at which corrosion occurs and C_{dl} is the corresponding capacitance. It will be noted that R_{por} can decrease due to a decrease of the coating resistance. The changes of

the impedance spectra are due to increases of R_{por} and R_{ct} with d increases. With increasing coating thickness the changes of the spectra in the low-frequency region become less pronounced. At high frequencies the data are dominated by electrolyte resistance while at very low frequencies the impedance is dominated by the oxide film resistance. At medium frequencies the capacitive behavior of the system is evident, determined by the dielectric properties of the naturally formed oxide film. A coating systems electrical ions and water penetration into the coating and subsequent electrochemical reactions at the polymer/metal interface.

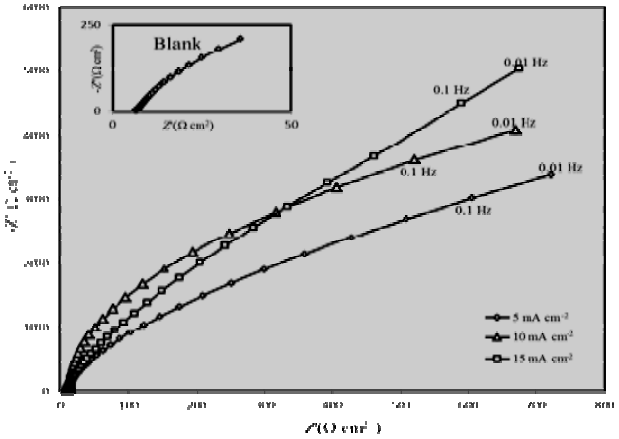

Fig. 9. Nyquist impedance plots for uncoated AA3004 and polyaniline-TiO_2 nanocomposite- coated AA3004 synthesized under galvanostatic conditions at various current densities ($mAcm^{-2}$) and the plots recorded at open circuit potential in aqueous solution of 3.5% NaCl.

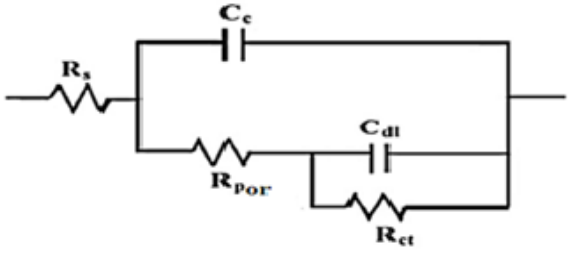

Fig 10. Equivalent circuit model.

The values of the polarization resistance can be determined using the equivalent circuit model by subtracting the pore resistance and solution resistance from total coating resistance. As it can be seen, the decline of impedance values in the lower frequency region can be interpreted as the delaminating of the coating, although the film was not physically detached from substrate metal surface in the microscopic sense. The increases in polarization resistance may be evaluated from Nyquist plot in low frequency region as shown in Fig. 8. The formation of pores in the paint film may also be estimated from reverse impedance values in low frequency region of Nyquist plot [46-48].

The values of the impedance parameters of the best fit to the experimental impedance plots for uncoated AA3004 and polyaniline-TiO_2 nanocomposite coated AA3004 with the equivalent circuits are given in Table 3. From the measured charge transfer resistance values, the protection efficiency of the coating was obtained from the following equation [39]: $PE = [(R_{corr(c)} - R_{corr}) / R_{corr(c)}]\times 100$ (3).

That $R_{ct(c)}$ and R_{ct} are the charge transfer resistance values in the presence and absence of polyaniline-TiO_2 nanocomposite coating, respectively. The R_{ct} value is approximately 51.2 $k\Omega\ cm^2$, which is about 15.5 times higher than that of uncoated AA3004. The higher value of R_{ct} is attributed to the effective barrier behavior of the polyaniline-TiO_2 nanocomposite coating. The lower values of C_c and C_{dl} for the polyaniline-TiO_2 nanocomposite-coated AA3004 provide further support for the protection of AA3004 by the polyaniline-TiO_2 nanocomposite coating.

Thus, the higher values of R_{ct} and R_{por} and lower values of C_c and C_{dl} indicate the excellent corrosion performance of the polyaniline-TiO_2

nanocomposite coating. The PE% calculated from EIS data is found to be 93.5%, which is in agreement with the potentiodynamic polarization results. It can be seen that the incorporation of TiO_2 nanoparticles into the polyaniline matrix exhibited better charge transfer resistances than for polyaniline-montmorrilonite and pure polyaniline-coated Al electrodes [28, 39]. The polyaniline-TiO_2 nanocomposite coating thickness on the surface AA3004 of the C_c can be achieved according to the following equation [43]: $C_c = \varepsilon_0 \varepsilon A d^{-1}$ (4). Where ε is the dielectric constant of the environment, ε_0 is the vacuum permittivity, A is the electrode area and d is the thickness of the protective layer. As can be seen in Table 3, the thickness for the uncoated electrode is aluminum oxide (Al_2O_3) and also with increasing applied current density increased thickness and reduced coating capacitance. The thickness is for polyaniline-TiO_2 nanocomposite coated AA3004 synthesized under galvanostatic conditions at 15 mA cm^{-2} current densities to the 6.36 μm.

4. Conclusion

The electrochemical synthesis of polyaniline-TiO_2 nanocomposite coating in aqueous solution containing oxalic acid and aniline monomers with dispersed TiO_2 nanoparticles on aluminum alloy 3004 substrates has been demonstrated. Electrodeposit uniform, compact and strongly adherent coatings can be obtained under galvanostatic condition. The polyaniline-TiO_2 nanocomposite coatings were characterized spectroscopically and the corrosion resistant properties of these electropolymerized films were evaluated using Tafel polarization and electrochemical impedance spectroscopy in 3.5% NaCl. The EIS results are in good agreement with the potentiodynamic polarization measurements. This study reveals that thepolyaniline-TiO_2 nanocompositecoating has excellent corrosion protection properties and can be considered a potential coating material to protect aluminum alloy 3004 against corrosion in aqueous 3.5% NaCl. The enhanced corrosion protection effect of the polyaniline-TiO_2 nanocomposite relative to pure polyaniline in the form of coating on metallic surface was attributed to the combination of the redox catalytic property of polyaniline and the barrier effect of the TiO_2 nanoparticles dispersing in the composite. We believe that the coating helps to stabilize the passive film onto the substrate thus stopping the metal dissolution.

Acknowledgment

The authors are grateful to University of Kashan for supporting this work by Grant No (159194/3).

References

[1] V. Karpagam, S. Sathiyanarayanan, G. Venkatachari, Curr. Appl. Phys. 8 (2008) 93-98.

[2] K. Kamaraj, S. Sathiyanarayanan, G. Venkatachari, Prog. Org. Coat. 64 (2009) 67-73.

[3] J. Huang, J. A. Moore, J. H. Acquaye, R. B. Kaner, Macromolecules. 38 (2005) 317-321.

[4] K. M. Cheung, D. Bloor, G. C. Stevens, Polymer. 29 (1988) 1709-1717.

[5] C. A. Ferreira, S. Aeiyach, M. Delammer, P. C. Lacaze, J. Electroanal.Chem. 284 (1990) 351-369.

[6] G. Troch Nagels, R. Winand, A. Weymeersch, L. Renard, J. Appl. Electrochem. 22 (1992) 756-764.

[7] F. Beck, R. Michaelis, J. Coat. Technol. 64 (1992) 59-67.

[8] F. Beck, R. Michaelis, F. Schloten, B. Zinger, Electrochim. Acta. 39 (1994) 229-234.

[9] S. Wenchang, J. O. Iroh, Electrochim. Acta. 46 (2000) 1-8.

[10] P. Ocon, F. A. B. Christobal, P. Herrasti, E. Fatas, Corros. Sci. 47 (2005) 649-662.

[11] B. R. W. Hinton, Met. Finish. 89 (1991) 55-61.

[12] P. Husler, F. Beck, J. Appl. Electrochem. 20 (1990) 596-605.

[13] F. Beck, P. Husler, J. Electroanal. Chem. 280 (1990) 159-166.

[14] S. B. Saidman, J. Electroanal. Chem. 534 (2002) 39-45.

[15] K. Naoi, A. Oura, M. Yoshizawa,M. Takeda, M. Ue, Electrochem. Solid State. Lett.
1 (1998) 34-36.

[16] K. Shah, J. O. Iroh, Adv. Polym. Techn. 23 (2004) 291-297.

[17] C. K. Tan, D. J. Blackwood, Corros. Sci. 45 (2003) 545-557.

[18] R. Rajagopalan, J. O. Iroh, Appl. Surf. Sci. 218 (2003) 58-69.

[19] M. S. Cho, S. Y. Park, J. Y. Hwang, H. J. Choi, Mater. Sci. Eng. 24 (2004) 15-18.

[20] S. Patil, J. R. Mahajan, M. A. More, P. P. Patil, S. W.Gosavi, S. A.Gangal, Polym. Int.
46 (1998) 99-105.

[21] L. H. Dao, M. Leclerc, J. Guay, J. W. Chevalier, Synth. Met. 29 (1989) 377-382.

[22] S. F. Patil, A. G. Bedekar, R. C. Patil, J. A. J. Kher, Mater. Sci. 32 (1997) 783-787.

[23] P. A. Kilmartin, G. A. Wright, Synth. Met. 104 (1999) 145-156.

[24] A. A. Athawale, S. F. Patil, B. Deore, Polymer. 40 (1999) 4929-4940.

[25]. J. Chevalier, J. Bergeron, L. H. Dao, Macromolecules. 25 (1992) 3325-3331.

[26] D. S. Lin, S. M. Yan, Synth. Met. 119 (2001) 111-112.

[27] A. Cook, A. Gabriel, D. Siew, N. Laycock, Curr. Appl Phys. 4 (2004) 133-136.

[28] M. Shabani-Nooshabadi, S. M. Ghoreishi, M. Behpour. Corr. Sci. 53 (2011) 3035-3042.

[29] O. Zubillaga, F. J. Cano, I. Azkarate, I. S. Molchan, G.E. Thompson, P. Skeldon, Thi. Sol. Film. 517 (2009) 6742-6746.

[30] Y. Zhu, J. O. Iroh, J. Adv. Mater. 34 (2002) 16-21.

[31] D. M. Lenz, C. A. Ferreira, M. Delamar, Synth. Met. 126 (2002) 179-182.

[32] G. Ciric-Marjanovi c, Synt. Meta. 170 (2013) 31-56.

[33] M.R. Mahmoudiana, Y. Alias, W. J. Basirun, M. Ebadi, Appl. Surf. Sci. 268 (2013) 302-311.

[34] M.R. Mahmoudian, W.J. Basirun, Y. Alias, Prog. Org. Coat. 71 (2011) 56–64.

[35] Y. Li, Y. Yua, L. Wua, J. Zhi, Appl. Surf. Sci. 273 (2013) 135-143.

[36] J. O. Iroh, Y. Zhua, K. Shah, K. Levine, R. Rajagopalan, T. Uyar, M. Donley, R. Mantz, J. Johnson, N. N. Voevodin, V. N. Balbyshev, A. N. Khramov, Prog. Org. Coat. 47 (2003) 365-375.

[37] A. Yagan, N. O. Pekmez, A. Yildiz, Electrochim. Acta. 51 (2006) 294-29559.

[38] K. C. Chang, S. T. Chen, H. F. Lin, C. Y. Lin, H. H. Huang, J. M. Yeh, Y. H. Yu, Eur. Polymer. J. 44 (2008) 13-23.

[39] M. Hamadanian, A. Reisi-Vanani, A. Majedi. Mat. Chem. Phys. 116 (2009) 376-382.

[40] M. Hamadanian, A. Reisi-Vanani, A. Majedi. Appl. Surf. Sci. 256 (2010) 1837-1844.

[41] M. Behpour, S. M. Ghoreishi, N. Soltani, M. Salavati-Niasari, M. Hamadanian, A. Gandomi, Corros. Sci. 50 (2008) 217-21812.

[42] M. Behpour, S. M. Ghoreishi, M. Salavati-Niasari, N. Mohammadi, J. Nanostructures, 2 (2012) 317-326.

[43] M. Shabani-Nooshabadi, S. M. Ghoreishi, M. Behpour, Electrochim. Acta. 54 (2009) 6989-6995.

[44] D. E. Tallman, K. L. Levine, C. Siripirom, V. C. Gelling, G. P. Bierwagen, S. G. Croll. Appl. Surf. Sci. 254 (2008) 5452-5459.

[45] S.M.Ghoreishi, M. Shabani-Nooshabadi, M. Behpour, Y. Jafari, Prog. Org. Coat. 74 (2012) 502- 510.

[46] F. Mansfeld, J. Appl. Electrochem. 25 (1995) 454 187–202.

[47] S. Gudic, J. Radosevic, M. Kliskic, Electrochim. Acta 47 (2002) 455 3009-3016.

[48] M.N. Jhon, H. Pham, Prog. Org. Coat. 27 (1996) 201–207.